Available online at www.sciencedirect.com
SCIENCE DIRECT®
International Journal of Heat and Mass Transfer 47 (2004) 5149–5157
International Journal of HEAT and MASS TRANSFER
www.elsevier.com/locate/ijhmt

Experimental investigation of heat-transfer characteristics of aluminum-foam heat sinks

W.H. Hsieh *, J.Y. Wu, W.H. Shih, W.C. Chiu

Department of Mechanical Engineering, National Chung Cheng University, Chia-Yi 621, Taiwan, ROC

Received 8 April 2004; received in revised form 22 April 2004
Available online 13 August 2004

Abstract

The demand of high speed and miniaturization of electronic components results in increased power dissipation requirement for thermal management. In this work, the effects of porosity (ε), pore density (PPI) and air velocity on the heat-transfer characteristics of aluminum-foam heat sinks are investigated experimentally. The phenomenon of non-local thermal equilibrium (NLTE) is also observed and reported. Results show that the *Nu* increases as the pore density increases, due to the fact that aluminum foam with a larger pore density has a larger heat-transfer area. The Nusselt number also increases with the increase of porosity due to the same reason. It is noted that temperatures of the solid and gas phases of the aluminum foam decrease as Reynolds number increases, caused by the increased convective heat-transfer rate at higher Reynolds number. The deduced temperature difference between the solid and gas phases clearly indicates the existence of non-local thermal equilibrium condition within the aluminum-foam heat sink. The increase of the porosity and the pore density enhances the phenomenon of non-local thermal equilibrium. The temperature difference increases with the decrease of Reynolds number and the distance away from the heat source.

Keywords: Porous material; Aluminum foam; Non-local thermal equilibrium; Nusselt number; Convective heat transfer

1. Introduction

The demand of high speed and miniaturization of electronic components results in increased power dissipation requirements for thermal management. Among various cooling techniques for electronic chips and/or modules, forced convective cooling with air features advantages of convenience and low cost [1]. Limitation of the forced convective cooling with air, however, lies in the relatively low heat removal rates. In the past, extensive studies have been conducted to improve the heat removal rate of forced convective cooling with air by utilizing heat sinks with different shapes, materials, flow patterns, etc. [2].

Metal-foam heat sinks made of copper or aluminum have proven to be appropriate for the cooling of high-power electronic components with excellent cooling performance under forced convective conditions [3–6]. Chao et al. [3] reported the thermal performance of a thermally enhanced plastic ball grid array (PBGA), which incorporates a heat slug in package, with a metal-foam heat sink on the top of the package. The measured results indicated a significant improvement

* Corresponding author. Tel.: +886 5 2428170; fax: +886 5 2720589.
E-mail address: imewhh@ccu.edu.tw (W.H. Hsieh).

0017-9310/$ - see front matter © 2004 Elsevier Ltd. All rights reserved.
doi:10.1016/j.ijheatmasstransfer.2004.04.037

Nomenclature

D	pipe diameter of the air inlet pipe, m
D_P	equivalent spherical diameter of porous media, m
d_p	mean pore diameter, m
f_k	friction factor of air flowing in aluminum foam
$\bar{h}$	mean convective heat transfer coefficient, W/m^2 °C
k	effective thermal conductivity, W/m °C
L	length of the test section, m
n	number of data points
Nu	Nusselt number
PPI	pores per inch
Re	Reynolds number
q	waste heat transfer rate, W
T	temperature, K
U	average entrance velocity

Greek symbols

μ	viscosity
ε	porosity
Δ	difference

Subscripts

air	air properties
e	estimate
f	fluid
in	inlet condition
I	electric current, A
s	solid
V	voltage
W	wall
∞	ambient condition

in power dissipation when a commercial pin-fin sink was replaced with an aluminum-foam heat sink under forced convective cooling condition. Chou and Yang [4] also showed the superior thermal-cooling performance of aluminum-foam sinks. At the air speed of 3.6 m/s, the overall heat transfer coefficient of aluminum foam with 91.4% porosity was reported to be 25% higher than that for conventional finned array. In Lee et al.'s [5] work, a dissipating power of 100 W for a 1 cm^2 chip with an aluminum metal-foam heat sink and a low-power muffin fan was demonstrated. Izadpanah et al. [6] showed the effect of natural convection is negligible and that forced convection is the main mechanism of heat transfer over range of operating condition in their investigation. In addition to the above-mentioned excellent cooling performance, the aluminum-foam heat sinks also feature the advantages of a small volume and light weight. The aluminum-foam heat sinks, nevertheless, have the disadvantages of a low mechanical strength, complicated manufacture processes, easy blockage by particles, etc.

In the convective cooling processes of electronic components with metal-foam heat sinks, the waste heat generated from electronic components goes through the metal foam, and then mostly dissipates convectively to the air (a small part of waste heat is transferred to the air by radiation). In engineering such a process, the heat-transfer characteristic, such as Nusselt number (Nu), is usually required. In this study, the Nu defined below is measured experimentally:

$$Nu = hL/k \tag{1}$$

and

$$h = q/[A(T_s - T_\infty)], \tag{2}$$

where h is the convective heat transfer coefficient, L, characteristic length, k, the effective thermal conductivity of the metal foam [7], q, the waste-heat transfer rate, A, the base area of a metal-foam heat sink, T_s, the surface temperature of waste-heat generating block, and T_∞, the temperature of the ambient air. In this paper, the Nusselt number is defined to evaluate the ratio of the convective heat transfer to the conductive heat transfer (including the conduction through the air and the aluminum) of the aluminum-foam heat sink. Thus, following the works by Bhattacharya and Mahajan [8] and Calmidi and Mahajan [9] the effective thermal conductivity, including the contributions from both conductivities of the air and aluminum, is used in Eq. (1) to calculate the Nusselt number. The effective thermal conductivity is a property evaluating the ability of the aluminum foam to conduct the heat through the gas (air) and solid (aluminum) phases of the aluminum foam under no flow condition.

In the theoretical study, the thermal analysis of metal-foam heat sinks has started to receive attention recently [9–12]. When analyzing the thermal performance of aluminum-foam heat sinks under forced convective conditions, it is well known that the assumption of local thermal equilibrium (LTE) between the air (the gas phase) and the solid metal matrix (the solid phase) usually leads to an unacceptable error in simulating heat transfer processes, due to the large difference in their thermal conductivities [13–17]. The deviation from the LTE condition is characterized by the temperature difference between the gas and the solid phases. Though the necessity of considering the temperature difference between the solid metal foam and the air has been demonstrated by various theoretical and numerical studies

discussed above, the experimental measurement of the temperature difference of the gas and the solid phases has yet to be performed to further investigate this phenomena and to provide data for model validation.

In this work, an experimental study is performed to measure the *Nu*, and the temperature distributions of the gas and the solid phases at the circumferential edge of six types of aluminum-foam heat sinks under forced convective cooling conditions. The effects of the porosity and the pore density of aluminum foam as well as the air velocity on *Nu* and the temperature distributions are also investigated in this work. In addition, the existence of NLTE condition within the aluminum-foam heat sink is also discussed based on the deduced temperature difference between the gas and the solid phases of aluminum-foam heat sinks.

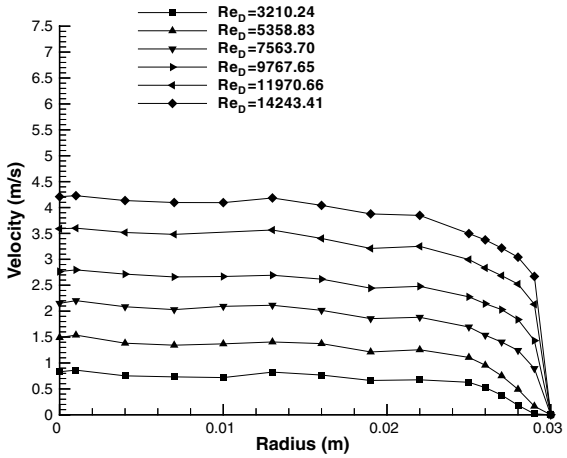

Fig. 2. Measured inlet velocity profile.

2. Method of approach

Fig. 1 shows the schematic diagram of the experimental apparatus used in this study for the measurement of heat-transfer characteristics of aluminum-foam heat sinks. The flow straightener within the inlet air pipe (diameter = 60 mm, length = 50 mm) consists of stacked foam sponges. In order to characterize the velocity profile of the air entering the aluminum foam, a hot-wire anemometer is used to measure the velocity profile. The velocity profiles measured at different Reynolds numbers are shown in Fig. 2. The definition of Re_D is

$$Re_D = \rho UD/\mu, \tag{3}$$

where D is the diameter of the air inlet pipe.

Fig. 2 shows that the velocity profiles of the air entering the aluminum-foam heat sink are uniform except near the wall of the pipe. It should be noted that the measurement of the velocity profile very near the wall region is not performed due to the difficulty in positioning the hot wire at the region. At the inlet of the aluminum foam, the temperature and pressure of the air are measured with a *k*-type thermocouple and a pressure transducer (Validyne pressure transducer, 0.5% accuracy), respectively, to determine the inlet air condition.

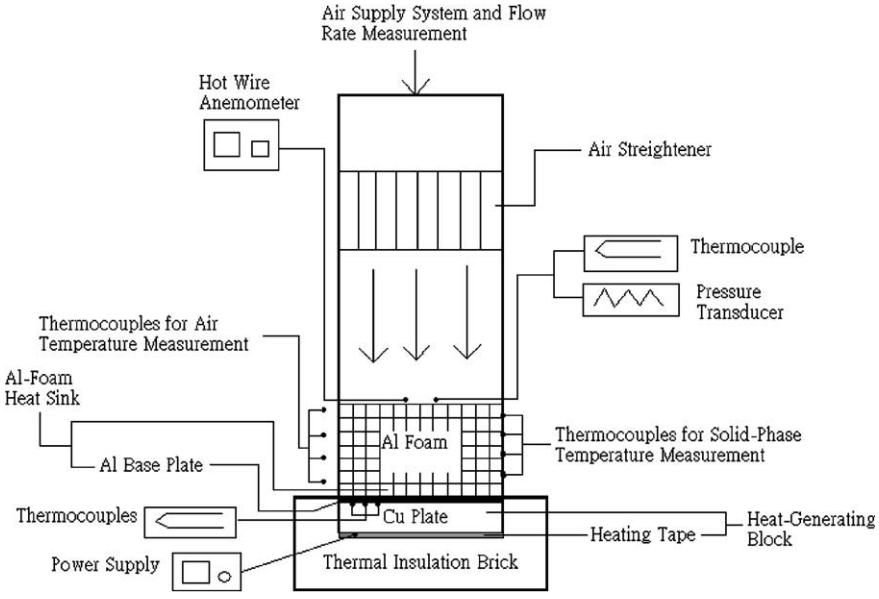

Fig. 1. Experimental apparatus for the measurements of heat transfer characteristics of aluminum-foam heat sinks.

Table 1
Properties of aluminum foam used in this study

Sample no.	PPI (pore/inch)	Porosity	Mean pore diameter, d_p (m)	Equivalent spherical diameter, D_P (m)	k_{eff} (W/m K)
1	10	0.92	1.19×10^{-3}	1.59×10^{-4}	5.89
2	20	0.87	8.27×10^{-4}	1.85×10^{-4}	8.32
3	20	0.91	8.05×10^{-4}	1.21×10^{-4}	6.34
4	20	0.94	8.14×10^{-4}	8.49×10^{-5}	4.95
5	20	0.96	8.00×10^{-4}	5.26×10^{-5}	3.55
6	40	0.94	6.85×10^{-4}	7.14×10^{-5}	4.50

Six types of aluminum-foam heat sinks as shown in Table 1 are used in this study. Samples 1, 4 and 6 are used for studying the pore-density effect, and 2–5, for porosity effect. The measurement of mean pore diameter (d_p) and equivalent spherical diameter (D_P) is achieved according to the method used in Refs. [18,19].

Each aluminum-foam heat sink is composed of a piece of aluminum foam and a base plate. The height and diameter of the aluminum foam are 60 and 65 mm, respectively. The base plate is made of 3-mm-thick aluminum. During tests, the waste heat is generated by a waste-heat generating block, which consists of a 20-mm-thick circular copper plate with a diameter of 65 mm and an electric heating plate, which is attached to the bottom of the copper plate as shown in Fig. 1. Three thermocouples for the measurement of T_s are placed in the groves at the top surface of the copper plate. Two thermocouples are installed at symmetric positions with respect to the center of the copper plate, and at a radius location 30 mm away from the center. The third one is also installed at 30 mm away from the center but at an angle of 90° from the direction formed by the other two thermocouples. Due to the highly conductive nature of the copper plate, the measured T_s from the three thermocouples are within 0.15%, and therefore, the values of T_s reported later in this paper are the average temperature of the T_s measured from the three thermocouples. In measuring the solid- and gas-phase temperatures of the heat sink, six k-type thermocouples are positioned at equal spacing along a z-direction line 0.1 cm away from the perimeter of the aluminum foam. These thermocouples measure the temperature profile of the air exiting the aluminum foam. Another set of six k-type thermocouples are silver-glued (also at equal spacing in the z-direction) at the perimeter of the solid-phase portion (aluminum portion) of the aluminum foam for the measurement of solid-phase temperature. During a test, the air flow is regulated by a valve, and straightened by the flow straightener installed in the air inlet pipe before entering the test section. While the valve is open, the power of heating tape is turned on, and the heat conducts to the porous heat sink through the copper plate. The readings of the thermocouples used to measure solid- and gas-phase temperatures are recorded when the steady-state condition has reached. The power of heating tape is then turned off, and the flow rate of air is increased to cool down the porous heat sink until it reaches the ambient temperature. This procedure is repeated for the six samples of porous heat sink at each flow rate. For examining repeatability of the experiments, the tests are repeated 3 times at each flow rate for samples 1 and 6. A good agreement is found in these tests at each air flow rate. The maximum difference in the measurement of the solid- and gas-phase temperature between these repeated tests is 4.8% and Nu, 2.4%. Due the demonstrated good repeatability of the experiments, one test is performed for the other samples at each flow rate.

In determining the convective heat transfer coefficient h, Eq. (2) is used with the substitution of measured T_s. In Eq. (2), q is the heat removed by the heat sink and is equal to the subtraction of heat loss through the thermal insulation brick to the ambient at the T_s from the waste heat generated by the heating tape. The heat loss through the insulation brick at different T_s is measured by the following procedures.

Fig. 3 shows the experimental apparatus for the measurement of heat loss through the insulation brick at different $(T_s - T_\infty)$, the experimental apparatus is the same as the one used for Nu measurement described above, except that the aluminum-foam heat sink is removed from the apparatus. As shown in Fig. 3, the heating tape is powered by a DC power supply. A FLUKE Hydra Series II records the top-surface temperature

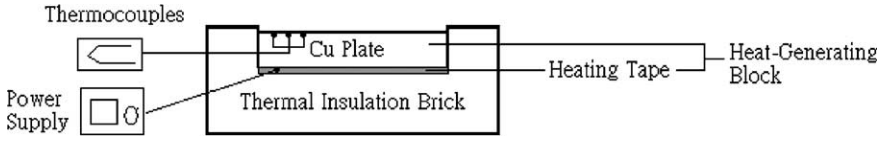

Fig. 3. Apparatus for measuring heat loss.

of the copper plate T_s and the ambient temperature T_∞. The copper plate and the heating tape are placed within the thermal insulation bricks made of alumina ($Al_2O_3 + Si_2O_2 + Fe_2O_3$, bulk density $\leqslant 0.9$ g/cm^3, porosity $\leqslant 0.8$, thermal conductivity at 350 °C $\leqslant$ 0.314 W/m °C). The temperatures of the top surface of the copper plate and the ambient are both measured under natural convection and steady-state condition. The heat loss through the insulation brick at different $(T_s - T_\infty)$ is calculated by the equations given below:

$$q_{loss} = q_{in} - q_{Natural\ convection}, \tag{4}$$

$$q_{in} = IV, \tag{5}$$

$$q_{Natural\ convection} = \bar{h}A(T_s - T_\infty), \tag{6}$$

where q_{loss} is the heat loss through the alumina brick to the ambient; $q_{Natural\ convection}$ is the heat transfer through natural convection from the top surface of the copper plate to the ambient; $\bar{h}$ is the average natural convective heat transfer coefficient at the top surface of the copper plate [20]; A is the top surface area of the copper plate; T_s is the top-surface temperature of the copper plate, which ranges from 317 to 380 K in this study; T_∞ is the temperature of the ambient; q_{in} is the power generated by the heating tape; I and V are the input DC current and voltage, respectively. The correlation between heat loss and temperature difference of the copper plate and ambient deduced from the experimental data is

$$q_{loss} = 1.26 \times 10^{-7}(T_s - T_\infty)^3 - 3.9 \times 10^{-6}(T_s - T_\infty)^2 + 7.61 \times 10^{-2}(T_s - T_\infty) + 0.179. \tag{7}$$

The standard error of estimate of the correlation is less than 5.8% [21]. In estimating the heat loss through the heat insulation brick in the measurement of heat-transfer characteristics of porous aluminum heat sinks, the measured T_s and T_∞ during an experiment are substituted into Eq. (7) to obtain the heat loss through the insulation brick. The result shows that the heat loss is a function of the temperature difference between the top surface of the copper plate and ambient, and the heat loss is about 9–18% of the input power.

3. Results and discussion

To analyze the heat-transfer phenomena of aluminum-foam heat sinks for electric devices, this work measures the temperature distributions of air and aluminum foam, and the surface temperature of the waste-heat generating block experimentally. Nusselt number and dimensionless temperatures are deduced from the experimental data.

Fig. 4 shows the effect of Reynolds number on Nu for heat sinks with different porosities. The pore densities

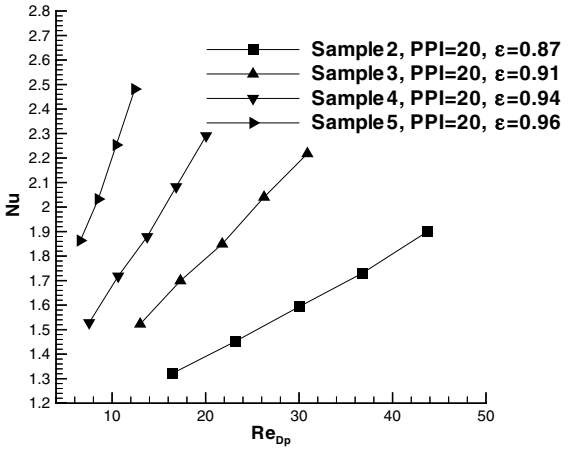

Fig. 4. Effect of Reynolds number on Nu for heat sinks with different porosities.

for the four samples are the same. The Reynolds number based on the equivalent spherical diameter and the Darcy velocity (which is equal to the average inlet velocity) is defined as

$$Re_{D_P} = \rho U D_P / \mu. \tag{8}$$

It could be seen in Fig. 4 that Nusselt number increases with the increase of Reynolds number. This is because the convective heat transfer increases with flow velocity. Fig. 4 also shows that Nusselt number increases with the increase of porosity. Fig. 5 shows the relation between Nusselt number and Reynolds number for three samples with different pore densities. It could be seen in Fig. 5 that Nusselt number increases with the increase of Reynolds number and the increase of pore density.

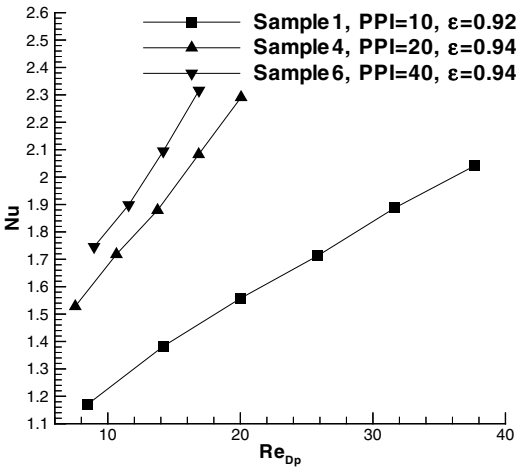

Fig. 5. Effect of Reynolds number on Nu for heat sinks with different pore densities.

Table 2
Coefficients of the correlations between Nu and Re_{D_p}

Sample no.	$Nu = aRe^b_{D_p}$		
	a	b	S_e
1	0.51	0.38	2.86×10^{-2}
2	0.45	0.38	3.35×10^{-2}
3	0.49	0.44	2.66×10^{-2}
4	0.64	0.42	3.96×10^{-2}
5	0.77	0.46	3.63×10^{-2}
6	0.63	0.46	3.80×10^{-2}

Based on the experimental results shown in Figs. 4 and 5, a correlation between Nusselt and Reynolds number for each sample is obtained by a least-square fitting method. The correlation is expressed in the form of the following equation:

$$Nu = aRe^b_{D_p}. \tag{9}$$

The coefficients, a and b, of Eq. (9) are tabulated in Table 2. The standard error of estimate, S_e, is defined as [21]

$$S_e = \sqrt{\sum_i^n (Nu_i - Nu_{\mathrm{pred},i})^2/(n-2)}, \tag{10}$$

where n is the number of data point, $n-2$ is the degree of freedom, Nu_i, the ith data point of measured Nusselt number, and $Nu_{\mathrm{pred},i}$, the calculated Nusselt number by Eq. (9). Fig. 6 shows the comparison of measured Nu and calculated Nu by Eq. (9) with a and b given in Table 2. The result shows hat the fit are in good agreement with measured Nu. Among the correlations for samples 1, 4, and 6, it is found that both a and b increase as the pore density is increased. Among the correlation for samples 2–5, it is found that the porosity affects a and b in the same manner.

In order to investigate the local thermal equilibrium condition of aluminum-foam heat sinks, the temperatures of solid and gas phases at the perimeter of the heat sinks are measured at different Reynolds numbers. The results are shown in Fig. 7. The dimensionless temperatures of the solid and gas phases are defined, respectively, as

$$\theta_s = (T_s - T_{in})/(qH/k), \tag{11}$$

$$\theta_f = (T_f - T_{in})/(qH/k), \tag{12}$$

where T_{in} is the inlet temperature of air.

In Fig. 7, it is found that the dimensionless temperatures are the highest at the bottom, and the lowest at the top, due to the fact the heat source is located at the bottom. At $z/H = 0.2$, when Reynolds number increases from 20.0 to 37.66, the dimensionless solid-phase temperature reduces from 0.37 to 0.22 and the dimensionless fluid temperature, from 0.19 to 0.08, caused by the enhanced heat transfer effect at higher velocity. When z/H is close to unity, the dimensionless solid- and gas-phase temperatures are both close to zero. It is also observed in Fig. 7 that the dimensionless solid and fluid temperatures are different from each other, which implies the existence of non-local thermal equilibrium condition between the solid and the gas phases.

The effect of the Reynolds number on the distribution of dimensionless temperature difference is presented in Fig. 8. The definition of the dimensionless temperature difference is given below:

$$\Delta\theta = \theta_s - \theta_f. \tag{13}$$

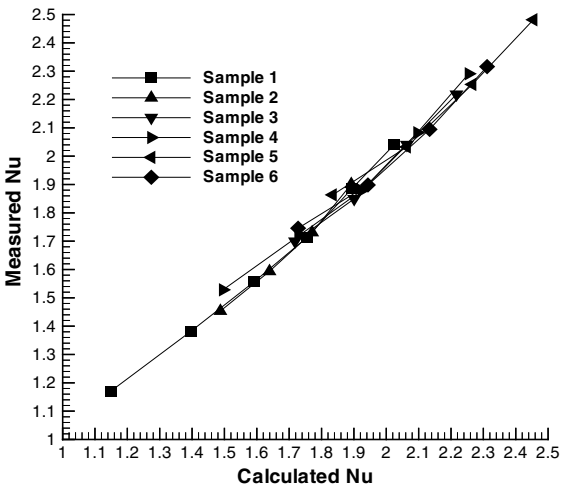

Fig. 6. Comparison of measured Nu and calculated Nu by Eq. (9) (a and b are given in Table 2).

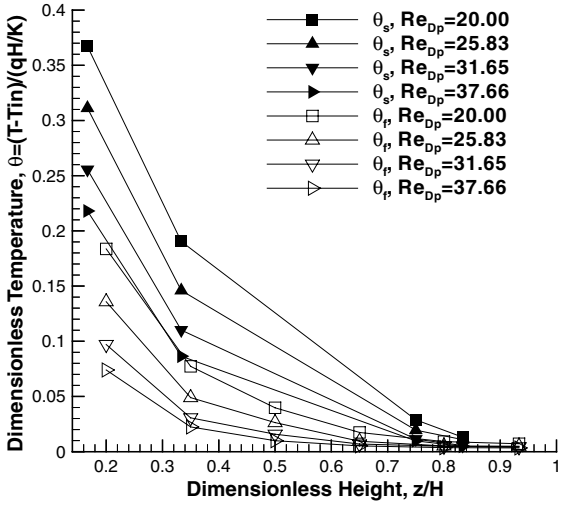

Fig. 7. Effect of Reynolds number on the distributions of dimensionless temperature of sample 1.

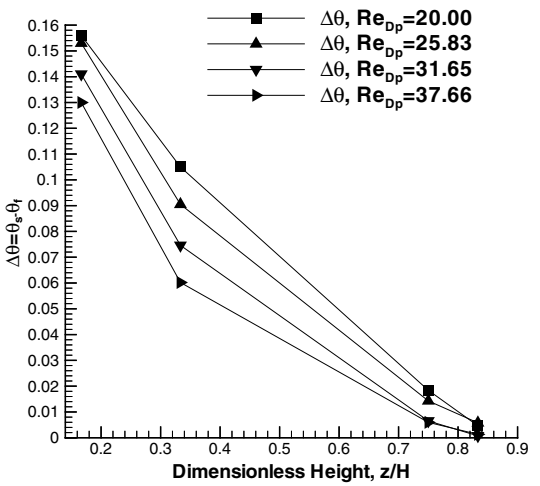

Fig. 8. Effect of Reynolds number on the distributions of dimensionless temperature difference of sample 1.

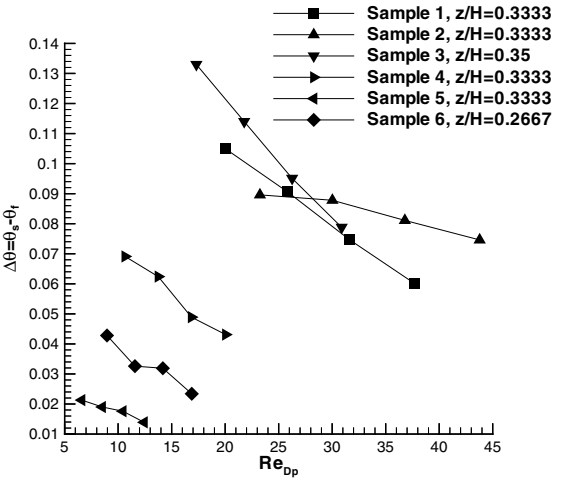

Fig. 9. Effect of Re_{D_p} on dimensionless temperature difference at $z/H = 0.35$.

Fig. 8 shows that the dimensionless temperature difference reduces when the Reynolds number increases from 20.0 to 37.66. This is because that the convective heat-transfer effect increases with the increase of Reynolds number which results in a reduced temperature difference between the air and the solid. When z/H approaches zero, the dimensionless temperature difference approaches a maximum under each test condition shown in Fig. 8, which indicates a strong non-local thermal equilibrium condition near the heat source located at the bottom of the heat sink.

Since the heat is conducted to metal-foam heat sink from the base plate, the heat exchange between the solid and the gas phases can be investigated by observing the temperature difference near the base plate. Fig. 9 shows that the effect of Reynolds number on the dimensionless temperature difference for all samples around $z/H = 0.35$. It appears that dimensionless temperature difference of all the six samples ranges from 0.01 to 0.14, and decreases with the increase of Reynolds number. Among samples 1, 4, and 6, the temperature difference in sample 1 is the largest, and the one in sample 6 is the least. It implies that the temperature difference between the solid and air decreases with the increase of pore density. Among samples 2–5, the temperature differences of samples 2 and 3 are close to each other and larger than samples 4 and 5. The temperature difference in sample 5 is the least. This indicated that the temperature difference between the solid and air decreases with the increase of porosity.

The Reynolds number and the spatial location, among others, are the two main factors affecting the local thermal equilibrium condition between the solid ant the air. Fig. 10 shows the effects of these two factors

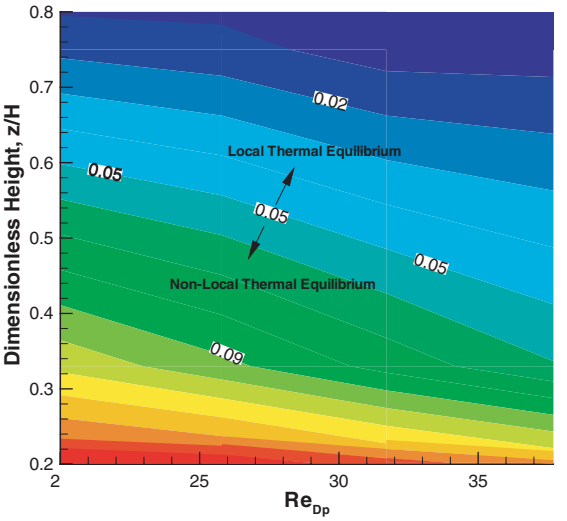

Fig. 10. The contour of dimensionless temperature difference of sample 1 plotted in the Reynolds number-dimensionless height coordinates.

on the difference of dimensionless temperatures. It is observed that the temperature difference decreases with the increase of Reynolds number and the dimensionless height. In modeling the heat-transfer processes of porous materials, according to Kambiz Vafai and Mehmet Sozen [22], the effect of non-local thermal equilibrium between the solid and the fluid should be considered when the temperature difference between the two phases exceeds 5%, and the assumption of local thermal equilibrium is no longer valid. According to this 5%

temperature difference, the boundary between the local thermal equilibrium regime and non-local thermal equilibrium regime is plotted in Fig. 10. It is noted that the local thermal equilibrium regime is located at the high Reynolds number and large dimensionless height (top/right) portion of the figure, and non-local thermal equilibrium regime, the low Reynolds number and small dimensionless height (low/left) portion of the figure.

4. Summary and conclusions

The summary and conclusions of this study are given below:

(1) The heat-transfer characteristics of aluminum-foam heat sinks are investigated experimentally in this work. A set of correlations between Nusselt number and Reynolds number for six types of aluminum-foam heat sinks is obtained experimentally. The values of a and b in the correlation both increase with the pore density and the porosity of aluminum-foam heat sink.
(2) Both the porosity and pore density affect the cooling performance of aluminum-foam heat sinks. The Nusselt number increases with the increase of the porosity and the pore density.
(3) The phenomenon of non-local thermal equilibrium between the solid- and gas-phases is observed to exist. The non-local thermal equilibrium condition diminishes with the increase of Reynolds number and the distance away form the heat source.
(4) The temperature difference between the solid and the gas phases decreases with the increase of the porosity and the pore density of aluminum-foam heat sinks. The increase of the porosity and the pore density also enhances the phenomenon of non-local thermal equilibrium.

Acknowledgment

This work represents part of the results obtained under contract no. NSC-90-2212-E-194-038 sponsored by National Science Council, Taiwan, ROC.

References

[1] S. Sathe, B. Sammakia, A review of recent development in some practical aspects of air-cooled electronic packages, Trans. ASME, J. Heat Transfer 120 (1998) 830–839.
[2] A. Bhattacharya, R.L. Mahajan, Finned metal foam heat sinks for electronics cooling in forced convection, J. Electron. Packag. 124 (2002) 155–163.
[3] C.-H. Chao, J.-M. Li, Foam-metal heat sinks for thermal enhanced BGA package applications, in: The Eleventh International Symposium on Transport Phenomena ISTP-II, vol. 4, Hsinchu, Taiwan, pp. 23–29.
[4] S.-F. Chou, C.-H. Yang, Heat transfer characteristics of aluminum foam metal, Proceedings of Sixth International Symposium on Transport Phenomena in Thermal Engineering, Seoul, Korea, 1993, pp. 709–714.
[5] Y.C. Lee, W. Zhang, H. Xie, R.L. Mahajan, Cooling of a FCHIP package with 100 W, 1 cm^2 chip, Proceedings of the 1993 ASME International Electronic Package Conference, vol. 1, ASME, New York, 1993, pp. 419–423.
[6] M.R. Izadpanah, H. Muller-Steinhagen, M. Jamialahmadi, Experimental and theoretical studies of convective heat transfer in a cylindrical porous medium, Int. J. Heat Fluid Flow 19 (1998) 629–635.
[7] V.V. Calmidi, R.L. Mahajan, The effective conductivity of high porosity fibrous metal foams, J. Heat Transfer 121 (1999) 466–471.
[8] A. Bhattacharya, R.L. Mahajan, Finned metal foam heat sinks for electronics cooling in forced convection, J. Electron. Packag. 124 (2002) 155–163.
[9] V.V. Calmidi, R.L. Mahajan, Forced convection in high porosity metal foams, J. Heat Transfer 122 (2000) 557–565.
[10] V.V. Calmidi, Transport Phenomena in High Porosity Fibrous Metal Foams, Ph.D. Thesis, Department of Mechanical Engineering, University of Colorado, 1998.
[11] B.V. Antohe, J.L. Lage, D.C. Price, Numerical characterization of micro heat exchangers using experimentally tested porous aluminum layers, Int. J. Heat Fluid Flow (1996) 594–603.
[12] J.L. Lage, A.L.D.C. Weinert, Numerical study of a low permeability microporous heat sink for cooling phased-array radar systems, Int. J. Heat Mass Transfer 39 (1996) 3633–3647.
[13] M. Sozen, K. Vafai, Longitudinal heat dispersion in porous beds with real gas flow, J. Thermophys. Heat Transfer 7 (1993) 153–157.
[14] A. Amiri, K. Vafai, Analysis of dispersion effects and non-thermal-equilibrium, non-Darcian, variable porosity incompressible flow through porous media, Int. J. Heat Mass Transfer 37 (1994) 939–954.
[15] G.J. Hwang, C.H. Chao, Heat transfer measurement and analysis for sintered porous channel, J. Heat Transfer 116 (1994) 456–464.
[16] G.J. Hwang, C.C. Wu, C.H. Chao, Investigation of non-Darcian forced convection in an asymmetric heated sintered porous channel, J. Heat Transfer 117 (1995) 725–732.
[17] W.H. Hsieh, S.F. Lu, Heat-transfer analysis and thermal dispersion in thermally-developing region of a sintered porous metal channel, Int. J. Heat Mass Transfer 43 (2000) 3001–3011.
[18] J.T. Richardson, Y. Peng, D. Remue, Properties of ceramic foam catalyst supports: pressure drop, Appl. Catal. A: General 204 (2000) 19–32.
[19] W.T. Wu, J.F. Liu, W.C. Chiu, W.H. Hsieh, Measurement and correlation of friction characteristic of flow through foam matrixes, Experimental Thermal and Fluid Science, submitted for publication.

[20] F.P. Incropera, Introduction to Heat Transfer, third ed., Wiley, 1996 p. 462.
[21] J.E. Freund, A. Gray, Simon Statistics—A First Course, sixth ed., Prentice-Hall, 1970 p. 455.
[22] K. Vafai, M. Sozen, Analysis of energy and momentum transport for fluid flow through a porous bed, J. Heat Transfer 112 (1990) 690–699.